Available online at www.sciencedirect.com

SciVerse ScienceDirect

Procedia Engineering 16 (2011) 499 – 505

Procedia Engineering

www.elsevier.com/locate/procedia

International Workshop on Automobile, Power and Energy Engineering

Subsurface Interfacial Defects of Metal Materials Testing Using Ultrasound Infrared Lock-in Thermography

Tang Qingju[a,b], Liu Junyan[a], Wang Yang[a*], Liu Hui[a]

[a]*School of Mechatronics Engineering, Harbin Institute of Technology, Harbin, 150001,China*
[b]*School of Mechanical Engineering, Hei Longjiang Institute of Science and Technology, Harbin, 150027, China*

Abstract

A novel non-destructive ultrasound infrared lock-in thermography (ULT) testing method was presented in order to detect metal specimens with subsurface contacting interfacial defects. An experimental platform was built. Experiments had been carried out to Q235 plates with different testing parameters. The testing effect of amplitude and phase images was analyzed, and the relation between amplitude difference, phase difference, signal-to-noise ratio and modulation frequency was discussed. An adaptive neuro-fuzzy inference system model was built to forecast the depth of defects.

Keywords: ultrasound infrared lock-in thermography; interfacial defects; amplitude; phase; modulation frequency

1. Introduction

Recently, the interest in the development of non-destructive testing technology is growing rapidly. The motivations behind it are to increase the testing efficiency to objects with different defects, such as inclusions, cracks, and interfacial defects [1-3].

With the objective of combination the advantages of ultrasound and infrared thermography, Busse. G proposed a novel ultrasound infrared lock-in thermography (ULT) testing method [4,5], which uses modulated ultrasonic wave to excite surface of a sample and lock-in method to process thermal image

* Corresponding author. Tel.: 045181056782.
E-mail address: tangqingju@126.com.

1877-7058 © 2011 Published by Elsevier Ltd. Open access under CC BY-NC-ND license.
doi:10.1016/j.proeng.2011.08.1116

sequence. D.Bates and G. Smith proved its efficiency to detect impact damage in aero composites [6,7]. Busse. G has done many experiments to inspect corrosion and delamination defects in aero plane components, and he illuminated ULT's broad application prospect in aerospace fields [8-10]. M.Y. Choi detected delamination defects inside timber by this method [11]. The deficiencies of the above research are as follows: (1) The relationship between testing efficiency and testing parameters while detecting interfacial defects hasn't been considered. (2) The qualitative research on the depth of defects is scarcely carried out.

The research contents and organization of the paper are as follows. In Section 2, the principle of ULT system is introduced. Section 3 indicates the preparation of specimens and experimental arrangements. In Section 4, test results are given and analyzed. An adaptive neuro-fuzzy inference system model is built to forecast the depth of defects in Section 5.

2. Detection principle

2.1. Principle of ULT system

Figure 1 shows the principle of the ultrasound infrared lock-in thermography testing system. After an amplitude modulation (AM) ultrasound emitted from the exciter head driven by signal generator and power amplifier is sent into the specimen with subsurface defects, the ultrasound at the interface of defects weaks and generates heat, due to the loss effect of mechanical energy or friction [12-14]. So varying temperature field on the surface of the specimen is formed through heat conduction. Then thermal changes on the surface are recorded with an infrared camera. Data is stored and processed by the computer through the Fourier transform, and the amplitude and phase images can be received. So defects can be detected by the amplitude and phase difference between defect and sound regions.

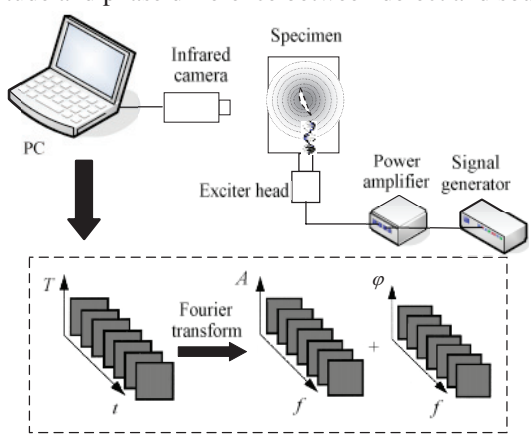

Fig.1 The principle of the ultrasound infrared lock-in thermography testing system

2.2. Infrared thermography sequence processing

An infrared thermography sequence can be captured by the infrared camera (for example, 320×240 pixels, et al.). Each frame of the sequence will be stored as an element of matrix $T(n)$, which can be expressed as

$$T(n)=\begin{bmatrix} T_{1,1}(n) & T_{1,2}(n) & \cdots & T_{1,320}(n) \\ T_{2,1}(n) & T_{2,2}(n) & \cdots & T_{2,320}(n) \\ \vdots & \vdots & \cdots & \vdots \\ T_{240,1}(n) & T_{240,2}(n) & \cdots & T_{240,320}(n) \end{bmatrix} \tag{1}$$

where n is the number of the frames, whose corresponding acquisition time is $t=n/f_s$; f_s is the sampling frequency; $T_{i,j}(n)$ means the temperature of i -line and j -column on the n -th frame.

Process $T(n)$ by Discrete Fourier Transform (DFT), yields

$$F(\mathrm{k})=\mathrm{DFT}[T(n)]=\sum_{n=0}^{N-1}T(n)e^{-j2\pi nk/N}=\sum_{n=0}^{N-1}T(n)W_N^{nk} \tag{2}$$

where W_N means the kernel function of DFT to n points, $W_N=e^{-j2\pi/N}$.

Fast Fourier Transform (FFT) is the fast algorithm of DFT . FFT can be used to analysis the spectrum of surface temperature signal or the infrared image sequences. Formula (1) shows that when the length of infrared image sequences is N , the baseband frequency signal of $f_0=1/t_0=f_s/N$ can be got with FFT , and by this, the harmonic amplitude and phase information of frequency kf_0 can be gained

$$A(k)=\left|F(k)\right| \tag{3}$$

$$\varphi(k)=\arctan(\frac{I_m[F(k)]}{R_e[F(k)]}) \tag{4}$$

3. Experiment design

An ULT experimental system is built and tests have been carried out. Four Q235 plates with defects varying in depth were made, using the internal contact interfaces in threaded connections to simulate the interfacial defects inside the materials. The specimens' surfaces were coated by matte black in order to increase the emissivity and reduce the reflectivity of the surfaces, and get accurate temperature signals. At room temperature, the standard atmospheric pressure and natural convection, tests were carried out under constant excitation position and initial static pressure to specimens, while different modulation frequencies were used. Test parameters are shown in table 1.

Table 1. Specimens and test parameters

Specimen No.	No. of defects	Defects depth h (mm)	Modulation frequency fm (Hz)
#S-1	3	4.40,5.50,7.50	0.1:0.1:0.3
#S-2	1	5.00	0.05:0.025:0.40
#S-3	1	6.20	0.05:0.025:0.25
#S-4	1	8.75	0.05:0.025:0.15

4. Test results and analysis

Figure 2 shows the amplitude and phase images of #S-1. Figure 2a) indicates the defects at h =4.4mm and 5.5mm can be tested with the modulation frequency f_m =0.1-0.3Hz, while the defect at h =7.5mm can only be tested with f_m =0.1-0.2Hz. Figure 2b) shows that all the defects can be tested, but the larger the modulation frequency, the noisier the phase image. Compared to amplitude images, phase images can detect much deeper defects.

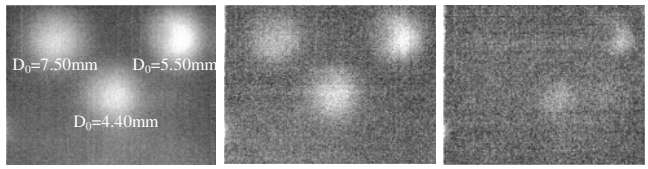

a) Amplitude images (left to right: f_m =0.1Hz, 0.2Hz, 0.3Hz)

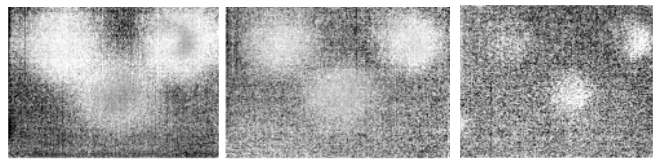

b) Phase images (left to right: f_m =0.1Hz, 0.2Hz, 0.3Hz)

Fig.2 Amplitude and phase images for inspecting samples with defects at different depth (# S-1)

The specimens #S-2, #S-2 and #S-3 are tested using the modulation frequencies in table 1. Figure 3 shows the corresponding amplitude and phase images, and all the defects can be detected with f_m =0.1Hz. The equation used in the calculation of the SNR (signal-to-noise ratio) was [15]

$$\begin{cases} SNR_{Ad} = \dfrac{|A_d - A_{nd}|}{\sigma_{And}} \\ SNR_{\varphi d} = \dfrac{|\varphi_d - \varphi_{nd}|}{\sigma_{\varphi nd}} \end{cases} \tag{5}$$

where SNR_{Ad} and $SNR_{\varphi d}$ represent the SNR of amplitude and phase images; A_d and φ_d are the means of amplitude and phase of defect regions; A_{nd} and φ_{nd} are the means of amplitude and phase of sound regions which at the fixed distance to defect regions. σ_{And} and $\sigma_{\varphi nd}$ are the mean amplitude and phase square deviations of the former sound regions.

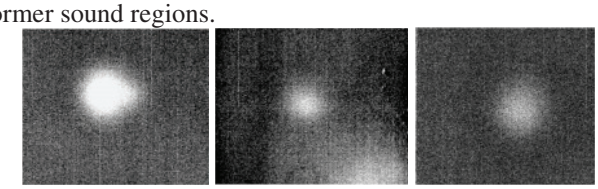

a) Amplitude images (left to right: #S-2, #S-2 and #S-3)

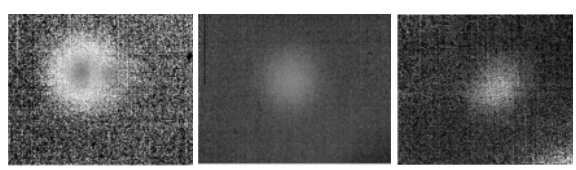

b) Phase images (left to right: #S-2, #S-2 and #S-3)

Fig.3 Amplitude and phase images for inspecting samples with defects at different depth (f_m =0.1Hz)

Figure 4 shows the relation between ΔA , $\Delta\varphi$, SNR(signal-to-noise ratio) and f_{m} , where ΔA and $\Delta\varphi$ mean the amplitude and phase differences between defect and sound regions. From figure 4 a) and b), with the increase of f_{m} , ΔA and image SNR_{Ad} decrease. A reduction in ΔA and SNR_{Ad} was also observed for the deeper defects while the same f_{m} . When f_{m} >=0.15Hz and h >=8.75mm, defects can not be tested. When f_{m} >=0.225Hz and h>=6.20mm, defects can not be tested. So lower f_{m} can be used to detect deeper defects. From figure 4 c) and d), with the increase of f_{m} , $\Delta\varphi$ and image $SNR_{\varphi\mathrm{d}}$ increase first and then decrease. A reduction in $\Delta\varphi$ was also observed for the deeper defects while the same f_{m} . When f_{m} >=0.175Hz, all $SNR_{\varphi\mathrm{d}}$ are very low. When f_{m} >=0.2Hz and h >8.75mm, defects can not be tested exactly. When f_{m} >=0.25Hz and h >5.00mm, defects can not be tested.

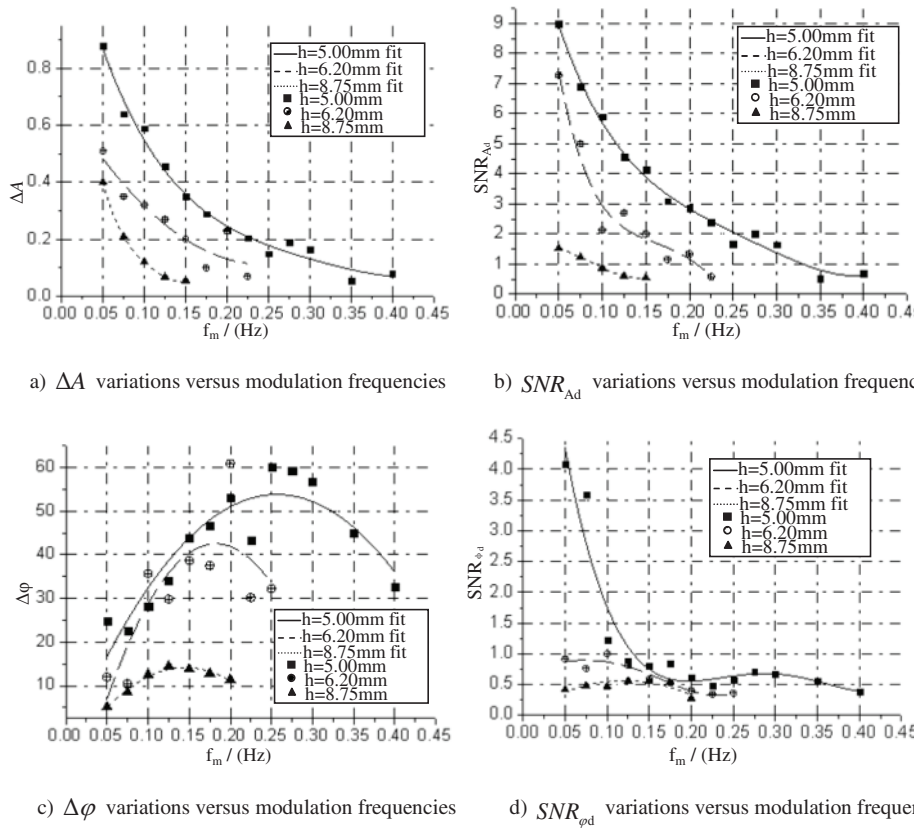

a) ΔA variations versus modulation frequencies b) SNR_{Ad} variations versus modulation frequencies

c) $\Delta\varphi$ variations versus modulation frequencies d) $SNR_{\varphi\mathrm{d}}$ variations versus modulation frequencies

Fig.4 Plots of results of detecting defects at different depth versus modulation frequencies

5. Detection determination of defects

Experimental studies have shown that phase images have a good ability of defects detection. φ_{d} is closely related to defect depth, and f_{m} is an important testing parameter affecting test effect. So the depth of defects can be determined as follows

$$h_{\mathrm{o}} = f(\varphi_{\mathrm{d}}, f_{\mathrm{m}}) \tag{4}$$

Fuzzy systems have the universal approximation properties. Jang combined Takagi-Sugeno and 5-layer neural network, and built ANFIS (Adaptive Neuro-Fuzzy Inference Stystem) [16]. The system can quickly complete highly nonlinear mapping, and has special advantages in system modeling. In this paper, f_m and φ_d as input, and defect depth h_o as output, and the test results as training samples, an ANFIS is built to forecast the depth of defects, shown in figure 5. Figure 6 shows the outputs of the networks (h_o) and exact depth (h_r).

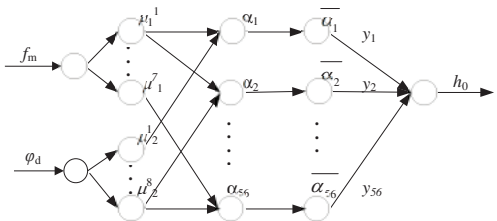

Fig.5 Structure of ANFIS model

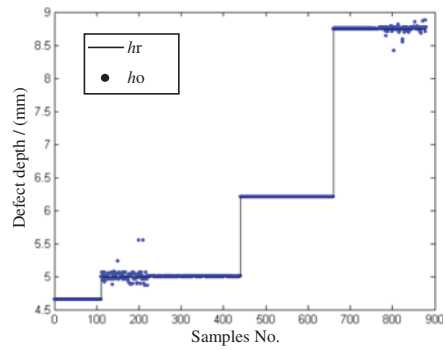

Fig.6 Outputs of the networks and exact depth

The built ANFIS is verified by test samples with defects varying in depth in table 2. The relative error between the predicted and actual results is lower than 5%.

Table 2. Results of determined depth and errors

f_m (Hz)	h_r (mm)	h_o (mm)	Error (%)
0.15	3.50	3.4739	0.75
0.175	5.00	4.8450	3.20
0.10	5.50	5.2580	4.90
0.10	6.20	6.1046	1.55
0.125	6.20	6.3056	1.70
0.125	8.75	8.5249	2.57

Conclusions

A novel non-destructive ultrasound infrared lock-in thermography (ULT) testing method has been described and the experimental system has been built. Specimens with interfacial defects of different depth are made and experimental results show the efficiency of ULT testing method to detect interfacial defects in metal materials. An adaptive neuro-fuzzy inference system model was built to forecast the depth of interfacial defects. The next study is to discuss the relationship between the excitation position, initial static pressure to specimens and the testing effect of ULT.

Acknowledgements

This work was financially supported by the National Natural Science Foundation of China (51074208).

References

[1] JaiWan Cho, ChinMan Chung and SeungHo Jung. Thermosonic Inspection of a Welded SUS Plate. Proc. of SICE-ICASE International Joint Conference. 2006, 1635-1639

[2] Jeremy Renshaw, Stephen D. Holland and Daniel J. Barnard .Viscous material-filled synthetic defects for vibrothermography. NDT&E International. 2009, 42:753-756

[3] Guo Xingwang, Ding Mengmeng. Simulation of Thermal NDT of Thickness and Its Uneveness of Thermal Barrier Coatings. ACTA AERONAUTICA ET ASTRONAUTICA INICA. 2010, 31(1):198-203(in chinese)

[4] G. Busse, M. Bauer, W. Rippel. Lock-In Vibrothermal Inspection of Polymer Composites. Quantitative Infrared Testing. 1992, 154

[5] J. Rantala, D. Wu G. Busse. Amplitude Modulated Lock-In Vibrothermography for NDE of Polymers and Composites. Research in Nondestructive Evaluation. 1996, 21(7)

[6] D. Betes, D. Lu, G. Smith; J. Hewitt. Rapid NDT of Composite Aircraft Components Using Lock-In Ultrasonic and Halogen Lamp Thermography. Proceeding of SPIE-The International Society for Optical Engineering. 2000, 3993:2-13

[7] D. Bates, G. Smith; J. Hewitt. Rapid Thermal Non-Destructive Testing of Aircraft Components. Composites Part B: Engineering. 2000, 31(3):175-185

[8] T. Zweschper, A. Dillenz, G. Riegert, D. Scherling, G. Busse. Ultrasound Excited Thermography Using Frequency Modulated Elastic Waves. Insight: Non-Destructive Testing and Condition Monitoring. 2003, 45(3):178-182

[9] G. Busse, A. Dillenz, T. Zweschper. Defect-Selective Imaging of Aerospace Structures with Elastic-Wave-Activated Thermography. Proceedings of SPIE-The international Society for Optical Engineering. 2001, 4360:580-586

[10] D. Wu, T. Zweschper, A. Salerno, G. Busse. Lock-in Thermography for Nondestructive Evaluation of Aerospace Structures. www.NDT.net

[11] M.Y. Choi, J. H. Park, W. T. Kim, K.S. Kang. Detection of delamination defect inside timber by sonic IR. Proceedings of SPIE - the International Society for Optical Engineering. 2008, 6939:69391F

[12] Xiaoyan Han, Md. Sarwar Islam. Finite element modeling of the heating of cracks during sonic infrared imaging. JOURNAL OF APPLIED PHYSICS. 2006, 99:1-7

[13] M.Y. Choi, J.H. Park and W.T. Kim. Detection of delamination defect inside timber by sonic IR. Proc. of SPIE. 2008, 6939:69391F

[14] Clemente Ibarra-Castanedo, Marc Genest and Stéphane Guibert. Inspection of aerospace materials by pulsed thermography, lock-in thermography and vibrothermography: A comparative study. Proc. of SPIE. 2007, 6541: 654116

[15] Deonna F. Woolard, K. Elliott Cramer. Line Scan Versus Flash Thermography: Comparative Study on Reinforced Carbon-Carbon. Proceedings of SPIE. 2005, 5782:315-323

[16] Takagi, M. Sugeno. Analysis and Design for a Class of Complex Control Systems Part I: Fuzzy Modeling and Identification. Automatica. 1997, 33(11):1017-1028